COBEM 2023 27TH INTERNATIONAL CONGRESS OF MECHANICAL ENGENEERING

ABCM Brazilian Society of Mechanical Sciences and Engineering
27th ABCM International Congress of Mechanical Engineering
December 04-08, 2023, Florianópolis-SC, Brazil

COB-2023-0421
A PROCEDURE BASED ON MULTIBODY DYNAMICS AND GENETIC ALGORITHM TO STUDY THE INFLUENCE OF THE HYDROPNEUMATIC SUSPENSION ON THE CABIN VIBRATION OF HAUL TRUCKS

Rodrigo Pessoa L. Oliveira
Marco Tulio C. Faria
Graduate Program in Mechanical Engineering, Federal University of Minas Gerais (UFMG), Av. Presidente Antônio Carlos 6627, Belo Horizonte, MG, 31270-901, Brazil.
rpl.oliveira@hotmail.com, mtfaria.ufmg@gmail.com

Abstract.
Many haul trucks subsystems are usually subjected to high levels of vibration during high-production mining. The vibration produced during the truck operation can compromise the drive ride comfort and health. The role played by the hydropneumatic suspensions is vital to reduce the level of transmitted vibration. In order to enlarge the knowledge about the influence of the suspension parameters on the truck dynamic behavior, firstly a ten degrees of freedom multibody dynamic model is developed. The source of vibration is based on standardized random functions associated with the road pavement quality. Some suspension experimental data are compared to the model results to check the model accuracy to reproduce actual conditions. Secondly, a multiobjective optimization procedure based on genetic algorithm is also implemented to generate some optimized suspension parameters that permit to reduce the cabin vibration, the chassis roll and the pitch angle. The results obtained indicate the significant influence of suspension parameters on both truck ride comfort and chassis movement behavior. For the truck CAT 775 considered in this study, the results rendered by the current parameters are close to the optimal point when evaluating the cabin acceleration separately. Nevertheless, with some adjustments and design parameter modifications, it would be possible to further enhance the dynamic behavior of chassis movement and even reduce slightly the cabin acceleration. However, even considering the optimal parameters, the analysis shows that the cabin vibration levels will be above the allowable limits for the truck using passive suspension running on roads with poor-quality profile.

Keywords: *Haul Trucks, Vehicle Ride Dynamics, Multibody Dynamics, Multiobjective Optimization, Genetic Algorithm.*

1. INTRODUCTION

Mining companies have been facing a problem of exposing ore truck drivers to whole-body vibration (WBV) levels exceeding the recommended values set by occupational health standards. The health problems caused by occupational exposure to vibrations in truck operations have led to the implementation of stricter standards regarding WBV levels for drivers of these vehicles. In Brazil, recent occupational health regulations have established tolerable levels of WBV for heavy vehicle drivers, necessitating enhanced monitoring and control of occupational vibration levels (Brasil, 2021).

The analysis of the various sources of vibration in trucks used for ore transport is essential to understand the parameters of mechanical subsystems (such as suspension, chassis, dump body and seat) that affect overall vibration levels. In recent years, there has been significant research on efficient vehicle suspension systems, with a particular focus on the development of hydropneumatic technologies.

For heavy-duty vehicles like ore trucks, hydropneumatic suspension (HPS) is commonly employed. HPS combines the advantages of hydraulic and pneumatic systems, providing a quick and precise response to road irregularities. Additionally, HPS allows for adjusting the stiffness and damping according to driving conditions, ensuring enhanced safety and comfort. Westhuizen and Els (2015) emphasize that heavy vehicles, such as ore trucks, often use HPS due to their high energy density and, therefore, smaller space requirements compared to conventional springs and dampers. Baldi and Meirelles (2003) highlight that cargo transport vehicles experience forces on their axles close to the allowed limits, mainly on rugged roads. In this case, the use of a conventional suspension system, where stiffness is constant, can increase the phenomenon of axle overload. The HPS, when used in these vehicles, offers the advantage of better load distribution per axle, reducing the problem of overload and increasing driving comfort.

Several studies have focused on haul truck dynamic and HPS behavior in recent years. Long et al. (2021) develop a ten degree of freedom computational model of a truck to evaluate vertical dynamics under various operating conditions, demonstrating the significant influence of road conditions on driving comfort. Kansake (2019) analyzes the dynamic forces imposed on roads by ore trucks, emphasizing the importance of considering these forces in road design. Ali and

Frimpong (2018) use artificial intelligence to model and predict real-time truck performance in order to enable the maintenance team to monitor the suspension performance and schedule maintenance effectively. Dindarloo (2016) studies the suspension aging impact on truck vibration level. The study considers both gradual effects, like hydraulic oil contamination, and sudden effects, such as road shocks. Results show significant increases in WBV levels over time. Wu et al. (2020) develop a computational fluid dynamics (CFD) model to evaluate the nonlinear characteristics of the HPS and determine damping and stiffness forces, considering the effects of oil temperature, oil viscosity, hydraulic oil and gas dissolution, and suspension vibration velocity.

Improving and optimizing suspension parameters to enhance ride comfort across various vehicle types have been also a subject of extensive research and some studies have focused on this area. Mitra et al. (2015) and Fossati and Miguel (2016) present simplified vehicle dynamic models using MATLAB/SIMULINK (The Mathworks, 2022). In their studies, multi-objective optimization techniques were applied using genetic algorithms to evaluate the trade-off between ride comfort and vehicle dynamic behavior and, therefore, obtain the optimal suspension parameters. Zhao et al. (2018) establish an optimization model using the particle swarm optimization algorithm to minimize vertical acceleration by optimizing HPS parameters (gas pressure, gas volume and damping valve diameter) of an articulated wheel loader.

The objective of this study is to analyze the HPS parameters influence on the ride comfort and also on the pitch and roll behavior of a mining truck CAT 775. A full vehicle vibration model with ten degrees of freedom based on Long et al. (2021) is developed. Nonlinear mathematical equations for stiffness and damping are established to determine the suspension forces. The complete model is developed and solved using MATLAB/SIMULINK. Firstly, the model is validated by comparing real gas pressure results with those obtained by the model. Secondly, a genetic algorithm technique is employed to perform a multiobjective optimization aiming at evaluating the trade-off between ride comfort and chassis moving behavior. The objective functions are the root-mean-square (RMS) values of the cabin vertical acceleration, chassis roll and chassis pitch angle. Eight suspension decision parameters (four for each axle) are considered in the optimization: initial gas pressure, initial gas volume, check valve ball diameter and damping valve orifice diameter.

2. VEHICLE VIBRATION MODEL

The vehicle vibration model is based on the free body diagram with ten degrees of freedom proposed by Long et al. (2021), as presented in Figure 1. There is one degree of freedom for each independent front axle vertical displacement (z_{af_1}, z_{af_2}) and two degrees of freedom for the dependent rear axle displacement and roll angle (z_{ar}, θ_{ar}). The cabin and the chassis have three degrees of freedom each one. The vertical and angular displacements of the cabin are represented by z_c, φ_c and θ_c, while the vertical and angular displacements of the chassis are represented by z_b, φ_b and θ_b.

The masses and inertias are denoted by m_{af_1} and m_{af_2} (front axles), m_{ar} and I_{arx} (rear axle), m_b, I_{bx}, and I_{by} (chassis), and m_c, I_{cx}, and I_{cy} (cabin). The stiffness and damping coefficients of the tires are represented by k_t and c_t, respectively. The HPS stiffness and damping coefficients are k_s and c_s. The stiffness and damping coefficients of the cabin suspension are represented by k_c and c_c. The excitation functions of the road surface are denoted by q_1, q_2, q_3, q_4, q_5, and q_6, which will be explained ahead.

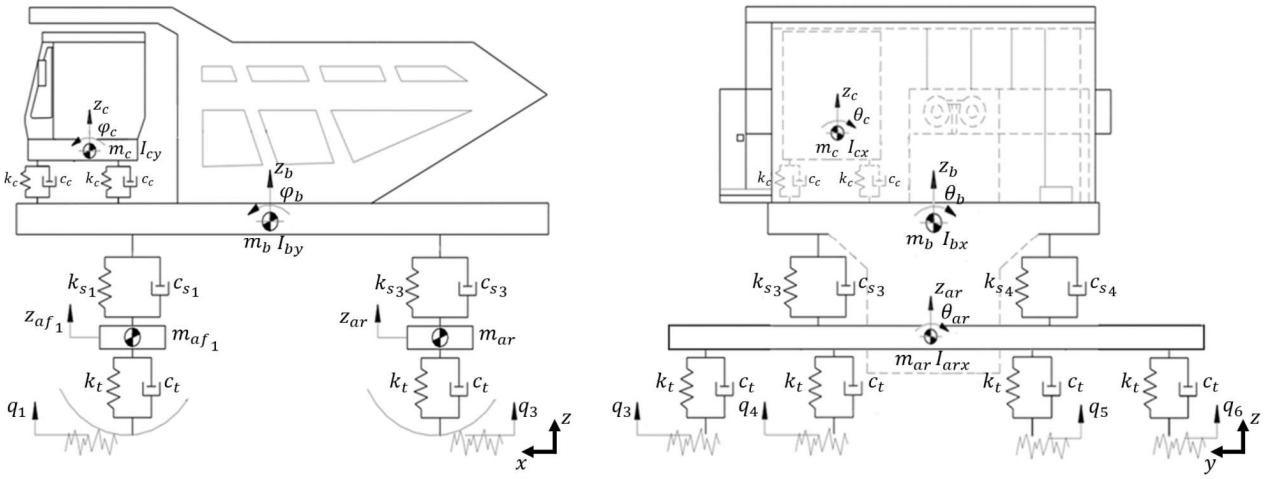

Figure 1. Free body diagram with ten degrees of freedom based on Long et al. (2021).

The ten equations of movement are developed based on D'Alembert's principle and in multibody dynamic theory. The differential equations are solved using the block diagram technique available on the SIMULINK.

2.1 Hydropneumatic suspension equations

The HPS consists of a main chamber filled with oil and gas, an annular chamber containing only oil, damping valves and check valves (unidirectional) between the two chambers. As it was deduced by Oscarsson (2015), the suspension total force (F_{int}) can be calculated as presented in Eq. (1), in which the first term represents the gas spring force while the second term which contains the pressure drop in the valves (ΔP) can be referred as the damping force. The pressure drop is presented in Eq. (2). The main chamber pressure and area are represented by P_1 and A_1, while for the annular chamber, P_2 and A_2.

$$F_{int} = P_1(A_1 - A_2) + \Delta P A_2, \tag{1}$$

$$\Delta P = P_1 - P_2, \tag{2}$$

2.1.1 Gas spring force

The HPS gas behavior modeling commonly relies on ideal gas theories, which have been effective in describing the system dynamics (Westhuizen and Els, 2015). Nitrogen (N_2) is commonly used in HPS due to its inert nature, no risk of explosion, and it is generally readily available. For nitrogen to behave as an ideal gas, it should operate at relatively low pressures and moderate to high temperatures. The polytropic process equation that represents the ideal gases change in state is shown in Eq. (3), where P_{g0} is the initial pressure, V_{g0} is the initial volume, P_{g1} is the pressure at a specific moment, V_{g1} is the volume at the same specific moment and r is the polytropic index (Bauer, 2011).

$$P_{g0}\,{V_{g0}}^r = P_{g1}{V_{g1}}^r, \tag{3}$$

From Eq. (3), the pressure at any specific moment can be described as presented in Eq. (4). Assuming the oil is an incompressible fluid, and the cylinder is a sufficiently rigid component, the gas volume at the same moment can be described by subtracting the volume displaced by the piston rod from the initial volume considering the cylinder completely extended, as presented by Eq. (5). The piston rod displacement is represented by x.

$$P_{g1} = \frac{P_{g0}{V_{g0}}^r}{{V_{g1}}^r}, \tag{4}$$

$$V_{g1} = V_{g0} - x(A_1 - A_2), \tag{5}$$

By combining the first term of suspension force general equation (Eq. (1)) with Eq. (4) and Eq. (5), it is possible to describe the gas spring force (F_{gas}), as presented in Eq. (6). The main chamber pressure P_1 is equal to the gas pressure P_{g1}.

$$F_{gas} = \frac{P_{g0}{V_{g0}}^r}{[V_{g0} - x\,(A_1 - A_2)]^r}\,(A_1 - A_2), \tag{6}$$

The value of the polytropic index (r) depends on the gas as well as the thermodynamic process involved. For an isothermal process with heat exchange and constant temperature, $r = 1$. Pure isothermal changes are suitable for slow loading scenarios, such as people entering or exiting a vehicle or payload loading and unloading. However, during vehicle operation, the suspension system needs to quickly absorb shocks, typically ranging from frequencies lower than 1 Hz to occasionally higher values than 10 Hz (Bauer, 2011). In such high-speed state changes, heat dissipation and absorption are limited, leading to a temperature change in the gas. In the absence of heat exchange, an adiabatic state change occurs, requiring the determination of the adiabatic index. According to standard literature, monatomic gases (e.g., He) have an adiabatic index of 1.66, while triatomic gases (e.g., CO_2) have an index of 1.30. Diatomic gases like nitrogen (N_2) and oxygen (O_2) have an adiabatic index of 1.40 under low pressures and ambient temperatures.

2.1.2 Oil damping force

A commonly used formulation to relate the pressure drop (ΔP_{res}) with the fluid flow rate through resistors (Q_{res}) is presented in Eq. (7), where ρ is the mass density of the oil, A_r is the area of the resistor, and C_d is the discharge coefficient of the resistor (Bauer, 2011).

$$\Delta P_{res} = \frac{\rho\,{Q_{res}}^2}{2\,(C_d A_r)^2}, \tag{7}$$

In the HPS case, the flow resistors are the damping and check valves that are installed in parallel between the two oil chambers. Therefore, the pressure difference for each damping valve (ΔP_{dv}) is equal to the pressure difference for each check valve (ΔP_{cv}), as presented in Eq. (8). The oil flow rate through each valve (Q_{dv} for the damping valve and Q_{cv} for the check valve) will be proportional to the resistance of the valve. The total oil flow rate (Q_t) is the sum of the flow rates through the valves and can also be obtained from the suspension displacement velocity ($\dot{x}$), as shown in Eq. (9). The damping and check valves quantities are q_{dv} and q_{cv}, respectively.

$$\Delta P = \Delta P_{dv} = \Delta P_{cv}, \tag{8}$$

$$Q_t = \dot{x} A_2 = q_{dv} Q_{dv} + q_{cv} Q_{cv}, \tag{9}$$

By combining Eq. (7), Eq. (8), and Eq. (9), it is possible to calculate the chambers pressure difference, and then obtaining the suspension damping force (F_{oil}), as presented in Eq. (10). When the suspension is in compression, $sign(\dot{x}) = 1$, and when it is in extension, $sign(\dot{x}) = -1$. Furthermore, when the suspension is in extension, the check valves are closed, meaning $q_{cv} = 0$. The valves discharge coefficient and area are $C_{d_{dv}}$ and A_{dv} (damping valve) and $C_{d_{cv}}$ and A_{cv} (check valve).

$$F_{oil} = \left(\frac{\dot{x} A_2}{q_{dv} C_{d_{dv}} A_{dv} + q_{cv} C_{d_{cv}} A_{cv}} \right)^2 \frac{\rho}{2} A_2 sign(\dot{x}), \tag{10}$$

2.2 Whole-Body Vibration

ISO 2631-1 (1997) is a very popular standard for measuring and evaluating human whole-body vibration. It employs two main criteria as presented in Eq. (11) and Eq. (12), namely the frequency-weighted RMS (a_{wrms}) and the vibration dose value (VDV), to describe the acceleration amplitude. The measurement duration is denoted by T, and $a_w(t)$ represents the frequency-weighted acceleration.

$$a_{wrms} = \sqrt{\frac{1}{T} \int_0^T a_w^2(t) dt}, \tag{11}$$

$$VDV = \sqrt[4]{\int_0^T a_w^4(t) dt}\,, \tag{12}$$

To evaluate the health risk associated with vibrations, ISO 2631-1 (1997) establishes the "Health Guidance Caution Zone" which relates exposure duration to weighted acceleration and classifies the risk level. For an eight-hour daily exposure, RMS weighted accelerations below 0.47 m/s² are considered low health risk, values between 0.47 m/s² and 0.93 m/s² are categorized as moderate health risk, and values exceeding 0.93 m/s² are classified as high health risk. The corresponding range limits values for the VDV measure are 8.5 m/s$^{1.75}$ and 17 m/s$^{1.75}$.

In this study, the basic evaluation method, which involves calculating the weighted acceleration RMS, is adopted. Nevertheless, some simplifications are considered. The effects of the operator seat and the frequency weighting are disregarded, and the evaluation of whole-body vibration considers solely the root-mean-square of the cabin vertical acceleration.

2.3 Road profile

The spatial random road surface roughness according to ISO 8608 (2016) is selected as excitation functions, which is defined as $q(x)$ by Eq. (13), where $G_d(n_i)$ is the power spectral density (PSD) for the spatial frequency n_i and can be calculated as presented by Eq. (14) considering the PSD for the reference spatial frequency $n_0 = 0.1\ m^{-1}$, presented as $G_d(n_0)$. Parameter Δn is the spatial frequency variation step and α_i is the phase of the harmonic function which is randomly generated between 0 and 2π. The spatial vector is defined as x_d.

Table 1 shows the reference $G_d(n_0)$ for different roads classes, which can provide the roughness degree of the road.

$$q(x) = \sum_{i=1}^{N} \sqrt{2 G_d(n_i) \Delta n}\, cos(2\pi n_i x_d + \alpha_i), \tag{13}$$

$$G_d(n_i) = G_d(n_0) \left(\frac{n_i}{n_0} \right)^{-2}, \tag{14}$$

Table 1. Degree of roughness for different roads classes (ISO 8608 (2016)).

Road Class	Degree of roughness $G_d(n_0)$[(1)] (10^{-6} m³)		
	Lower limit	Geometric mean	Upper limit
A	-	16	32
B	32	64	128
C	128	256	512
D	512	1024	2048
E	2048	4094	8192
F	8192	16384	32768

[(1)] $n_0 = 0.1\ cycles/m$.

2.4 Model validation

The gas pressure results obtained from the model for the four suspensions are compared with measurements taken from an actual CAT 775 truck in order to validate the model. The suspension parameters used in the validation process are the current values presented in Table 2. The polytropic index considered is 1.40, representing an adiabatic process. The valves discharge coefficient is 0.70, that was estimated based on the results presented by Wu et al. (2020). It is considered also a constant oil mass density of 994 kg/m².

Table 2. Current front and rear suspensions parameters (CAT 775).

Suspension parameter	Front	Rear
Initial gas pressure with fully extended suspension (P_{g0})	2600 kPa	1800 kPa
Initial gas volume with fully extended suspension (V_{g0})	5.18 L	3.11 L
Check valve orifice large diameter (D_{cv_max})	19.05 mm	19.05 mm
Check valve ball diameter (D_{ball})	15.9 mm	15.9 mm
Check valves quantity (q_{cv})	1	1
Damping valve orifice diameter (D_{dv})	4.5 mm	7.3 mm
Damping valves quantity (q_{dv})	2	1
Main chamber area (A_1)	0.03246 m²	0.03663 m²
Annular chamber area (A_2)	0.00765 m²	0.01181 m²
Maximum stroke (x_{HPS})	234 mm	149 mm

Due to the limited data acquisition frequency of the truck monitoring system, a sample of 1500 seconds is chosen to allow the comparison with the model predictions. The model employs a total time of 100 seconds. The validation process is performed by comparing the gas pressure root-mean-square (RMS) values. The $G_d(n_0)$ parameter used to generate the road profiles is adjusted to approximate the field and model data. Its value is assumed to be 2000 x 10^{-6} m³, generating road conditions between classes D and E, that represent a poor-quality road as presented in Table 1.

The comparison is conducted for the empty (no ore load) and the full loaded conditions (ore load of 64 t). According to the measurements at empty conditions, the truck speed varies around 30 km/h, and this value is assumed constant in the model. For the loaded condition, a constant speed of 20 km/h is considered also based on real data. Since the model time sample is considered the same for both profiles, the total traveled distances are different. The calibrated road profiles on the time domain for both cases are presented in Figure 2 for the early 30 seconds. The rear road profiles are offset from the front axle due to the truck wheelbase distance. Besides that, it is considered a correlation between the right and left profiles, as can be seen in the curves.

Figure 3 presents the measured and predicted results for the gas pressure varying on time for the empty and for the loaded condition, while Table 3 presents the comparison among the RMS values of the gas pressure.

By analyzing the curves and gas pressure RMS values, it is observed a good agreement among the measurements and the model predictions for the HPS gas pressure. However, some asymmetry is observed on the experimental results, whereas the predictions are practically symmetrical between truck sides. The observed asymmetry in the measured data can be referred to differences in adjustments between the suspensions, neglected road inclination, or variations of the load distribution carried by the truck, among other factors. The model assumes symmetry in the truck parameters (such as tire, suspension, mass, etc.) and regular material distribution, resulting in almost symmetric gas pressure between the truck sides. Therefore, despite the asymmetry on the gas pressure measures, it can be assumed that the model is capable of representing the truck dynamic behavior.

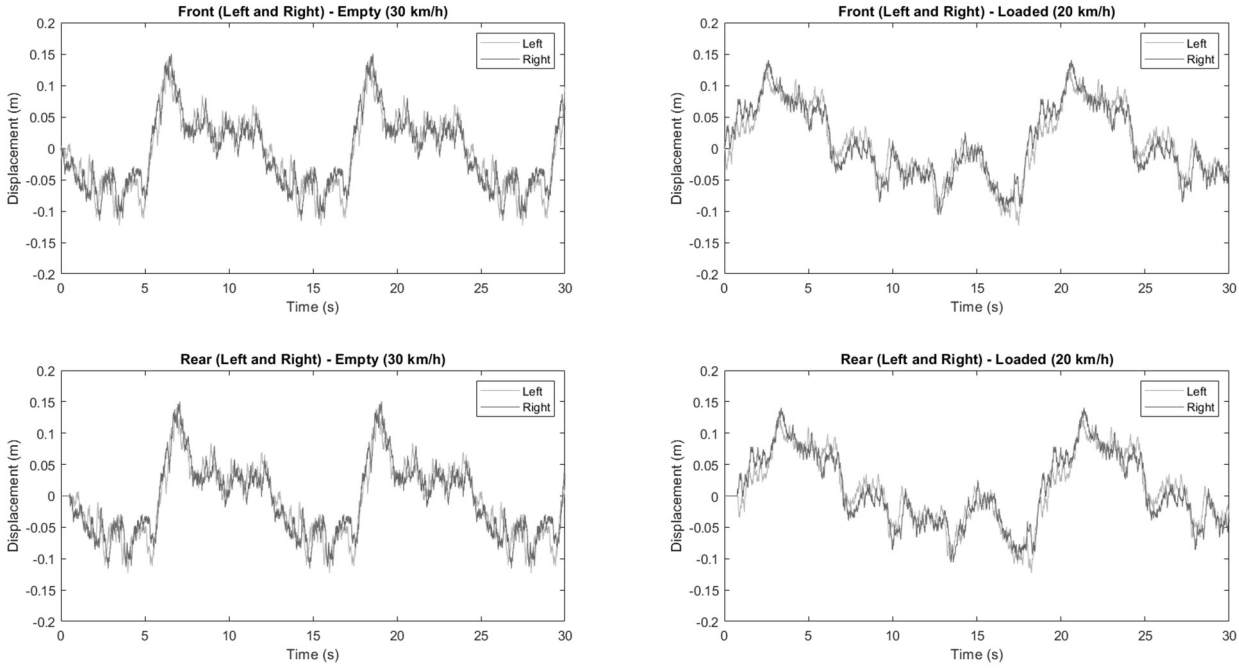

Figure 2. Calibrated road profiles on the time domain.

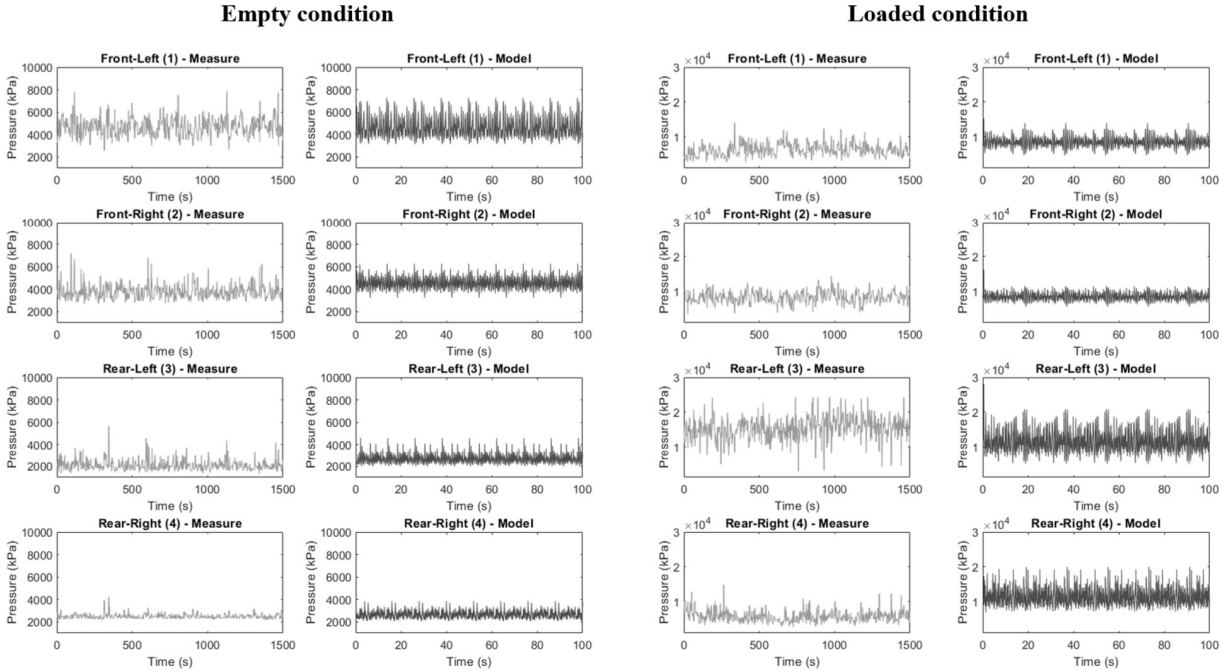

Figure 3. Comparison among measurements and predicted results for the gas pressure.

Table 3. Comparative RMS values for the gas pressure measurements and predictions.

Suspension	Empty		Loaded	
	Measure	Model	Measure	Model
Front-Left	4767 kPa	4644 kPa	6626 kPa	8518 kPa
Front-Right	3834 kPa	4526 kPa	8560 kPa	8464 kPa
Rear-Left	2170 kPa	2690 kPa	15775 kPa	11532 kPa
Rear-Right	2514 kPa	2658 kPa	6117 kPa	11359 kPa

3. DEFINING THE OPTIMIZATION PROBLEM

The optimization problem typically involves the following elements: objective functions, decision variables and boundary conditions.

3.1 Objetive functions

The objective functions for this multiobjective optimization study are the RMS values for the cabin vertical acceleration, the chassis roll angle and the chassis pitch angle. To obtain these three values, the SIMULINK model is employed for the unloaded (0 t) and loaded truck (64 t). The overall RMS values are then obtained to represent a truck operation cycle.

Evaluating whole-body vibration and ride comfort, the objective is to minimize the cabin vertical acceleration. In evaluating the truck lateral and longitudinal dynamic behavior, the objective is to reduce the chassis roll and pitch angles.

3.2 Decision variables

This work studies the global optimization problem with four decision variables for each truck axle, resulting in a total of eight decision variables. They are:

- Initial suspension gas pressures (P_{g0f}, P_{g0r}), that influence the suspension stiffness curves.
- Initial suspension gas volumes (V_{g0f}, V_{g0r}), that influence the suspension stiffness curves.
- Check valve ball diameters (D_{ballf}, D_{ballr}), that influence the suspension damping curves.
- Damping valve orifice diameters (D_{dvf}, D_{dvr}), that influence the suspension damping curves.

The gas initial volume and pressure are based on a suspension configuration for fully extended condition. The other suspensions data are presented in Table 2.

3.3 Boundary conditions

The boundary conditions are selected for the decision variables based on the feasible operating and geometric characteristics, considering the actual suspension parameters presented on Table 2. Some values are obtained by simple adjustment in the current truck CAT 775 suspensions. Other values involve a suspension design change. The same variable ranges are applied to both the front and rear suspensions, that are described below:

- 1000 kPa $\leq$ P_{g0f}, P_{g0r} $\leq$ 3000 kPa.
- 2.5 L $\leq$ V_{g0f}, V_{g0r} $\leq$ 6.0 L.
- 14 mm $\leq$ D_{ballf}, D_{ballr} $\leq$ 18 mm.
- 3 mm $\leq$ D_{dvf}, D_{dvr} $\leq$ 9 mm.

In addition to these constraints on the decision variables, the axial motion of the suspension (x_{HPSf} and x_{HPSr}) is also limited to:

- 0 mm $\leq$ $x_{HPSf}, x_{HPSr} \leq$ 250 mm.

3.4 Multiobjective optimization based on genetic algorithm

In a multiobjective optimization problem, multiple objective functions need to be optimized simultaneously, and there is not necessarily a solution that is better in relation to all objectives due to differences between the objectives. A solution can be better for one objective but worse for another. Therefore, there generally exists a set of solutions for the multiple objectives. For such solutions, called Pareto optimal solutions or non-dominated solutions, no improvement is possible in any objective function without sacrificing at least one of the other objective functions (Deb, 2011). The set of Pareto optimal solutions, when plotted in space, is known as the Pareto frontier. Identifying a set of Pareto optimal solutions is therefore crucial for a decision maker to choose a compromise solution that best satisfies the objectives. Choosing an optimized solution for only one objective may overlook solutions that are better from a general point of view. The set of Pareto optimal solutions defines this overall perspective (Thomann and Eichfelder, 2019).

In this study, it is employed the *gamultiobj* function from MATLAB to obtain the Pareto frontier. This function uses a controlled elitist genetic algorithm, which not only prioritizes individuals with superior fitness but also promotes diversity within the population. Maintaining diversity is crucial for converging towards an optimal Pareto frontier.

4. RESULTS AND DISCUSSIONS

The cabin vertical acceleration and the chassis roll and pitch angles are obtained at both the empty and loaded condition representing one operation cycle. The considered road profile for both conditions is that calibrated in the validation process presented in Figure 2, in which $G_d(n_0)$ is 2000 x 10^{-6} m³ and no elevation is considered in the circuit. To reduce the computer time in the optimization process, it is considered for both conditions a total travel time of 50 seconds. The truck speeds are 30 km/h for the empty condition and 20 km/h for the loaded condition.

A lane change maneuver is considered at the middle of the time interval for each stretch in order to represent various haul truck movements, such as evading obstacles, overtaking other vehicles, or adjusting to changes in the road alignment, as proposed by Prem (1998). To calculate the chassis lateral moment, a maximum lateral acceleration of 0.1 g is considered. The maneuver total time is 8 seconds. Besides the lateral acceleration the analysis also considers the longitudinal acceleration of starting and braking. To compute the longitudinal chassis moments, the acceleration of 0.2 g for both conditions is considered based on consistent speed change times and distances.

The genetic algorithm technique employs a population size of 400 individuals and 30 generations. The resulting Pareto frontier is illustrated in Figure 4, with key points of interest emphasized. Point R represents the reference point, corresponding to the current suspension system parameters (Table 2). The equilibrium point, denoted by an asterisk as Point E, represents the minimum values of the three objective functions. However, achieving this ideal point is unattainable. Therefore, the optimal Pareto frontier point (Point O) is the one that closely approximates the equilibrium point. Furthermore, there are highlighted the optimal points for individual optimizations: vertical cabin acceleration (Point A), chassis roll angle (Point B), and chassis pitch angle (Point C).

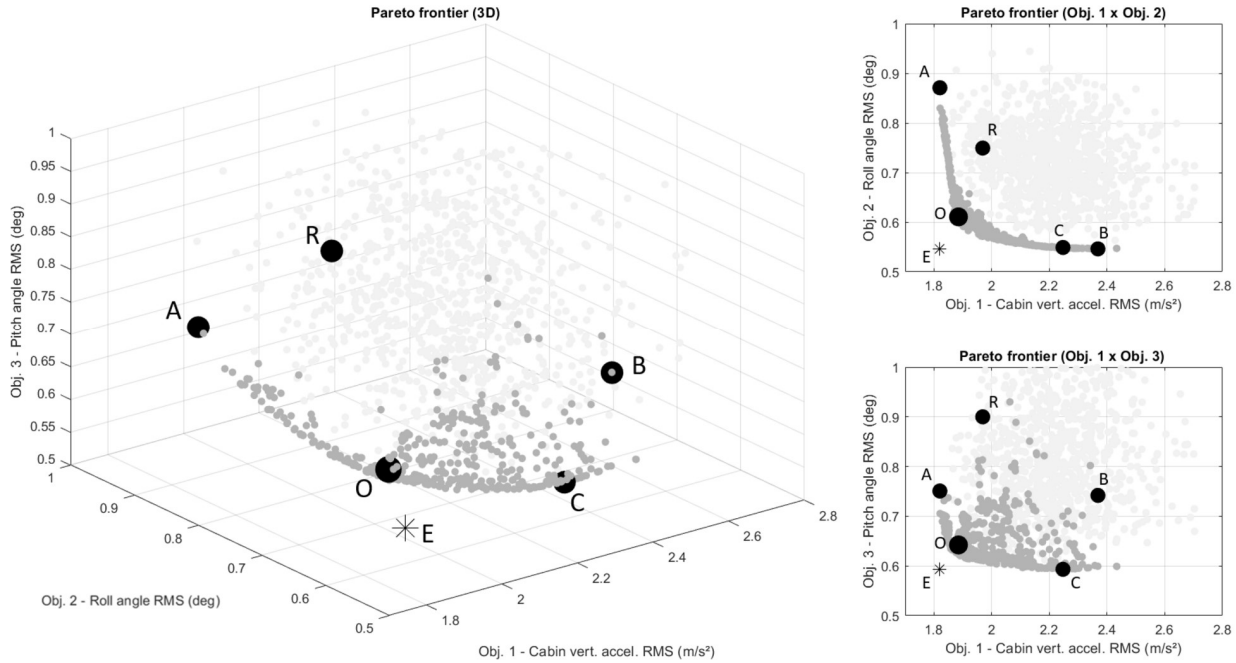

Figure 4. Pareto frontier with key points of interest.

Table 4 summarizes the results obtained values for the decision variables, as well as the key results for the five highlighted points in Figure 4. The coordinates of the equilibrium point (Point E) are as follows: 1.82 m/s² (cabin vertical acceleration RMS), 0.55 deg (chassis roll angle RMS), and 0.59 deg (chassis pitch angle RMS).

At Point A, the cabin vertical acceleration RMS exhibits the highest reduction compared to the reference Point R, with a decrease of approximately 8%. Additionally, the chassis pitch angle RMS also decreases by approximately 17%. Conversely, the chassis roll angle RMS increases by around 16%.

At Point B, the chassis roll angle RMS displays the most significant reduction compared to the reference Point R, with a decrease of approximately 27%. Moreover, the chassis pitch angle RMS also decreases by approximately 18%. However, the cabin vertical acceleration RMS increases by about 20%.

At Point C, the chassis pitch angle RMS exhibits the highest reduction compared to the reference Point R, with a decrease of approximately 34%. Similarly, the chassis roll angle RMS decreased by approximately 27%. Conversely, the cabin vertical acceleration RMS increases by about 14%.

Table 4. Results summarized for the key points of interest.

Parameter	Unit	Point R	Point O	Point A	Point B	Point C
Initial gas pressure (front)	kPa	2600	2739	2741	1001	2036
Initial gas pressure (rear)	kPa	1800	1100	1545	1000	1015
Initial gas volume (front)	L	5.18	5.95	5.96	3.50	3.00
Initial gas volume (rear)	L	3.11	3.67	5.49	2.75	2.82
Check valve ball diameter (front)	mm	15.9	18.0	18.0	14.5	16.6
Check valve ball diameter (rear)	mm	15.9	16.3	16.8	14.0	14.6
Damping valve orifice diameter (front)	mm	4.5	4.2	4.7	3.0	3.1
Damping valve orifice diameter (rear)	mm	7.3	3.2	7.5	3.0	3.0
Cabin vertical acceleration RMS	m/s²	1.97	1.89	1.82	2.37	2.25
Chassis roll angle RMS	deg	0.75	0.61	0.87	0.55	0.55
Chassis pitch angle RMS	deg	0.90	0.64	0.75	0.74	0.59
Maximum suspension stroke (front)	mm	157	175	176	129	99
Maximum suspension stroke (rear)	mm	109	136	196	103	106

Finally, in comparison to Point R, the optimal Point O indicates reductions in all three objective functions. The reduction in cabin vertical acceleration RMS is not significant (approximately 4%), suggesting that the current suspension parameters are close to the optimal point for this specific objective function. However, there estimated substantial reductions of 19% and 29% in the chassis roll and pitch angles, respectively. Figure 5 illustrates the comparison between Point O and Point R for the curves of cabin vertical acceleration, chassis roll angle, and chassis pitch angle. The differences are minimal for cabin vertical acceleration, while they are more noticeable for the chassis roll and pitch angles.

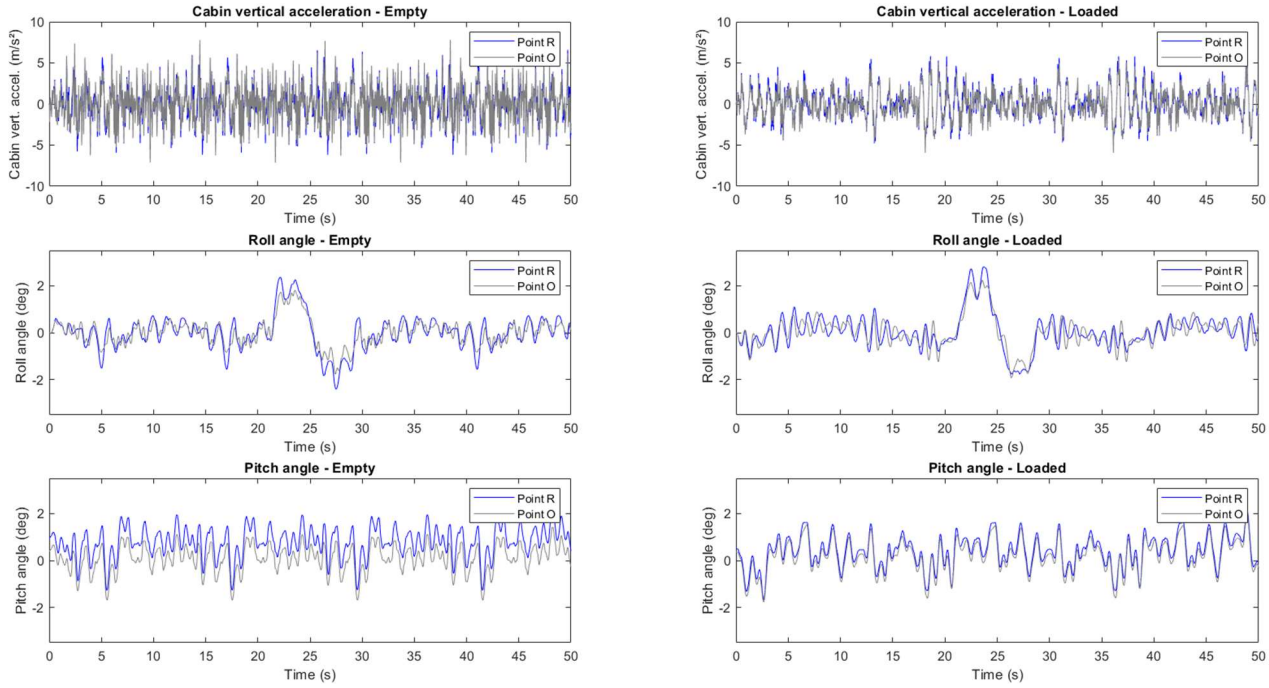

Figure 5. Comparative curves of cabin acceleration and chassis roll and pitch angles (Point R and Point O).

5. CONCLUSIONS

This study shows the development of a mining truck vibration model to analyze the effects of HPS parameters on cabin vertical acceleration and chassis movement behavior. The model has been validated by comparing the gas pressure predictions with experimental data. A multiobjective optimization is conducted, with the RMS of cabin vertical acceleration, chassis roll angle, and chassis pitch angle serving as objective functions. The Pareto frontier is obtained, and the following conclusions can be drawn from the results rendered for the truck CAT 775 suspension parameters.

(1) The HPS parameters have a significant influence on both truck ride comfort and chassis movement behavior.
(2) The cabin vertical acceleration RMS can be reduced by a maximum of 8%, but it will increase chassis movement. The chassis roll angle RMS can be reduced by maximum of 27%, and the chassis pitch angle RMS can be reduced by a maximum of 34%, but both will result in an increase in cabin acceleration. These are the maximum

achievable individual optimization values when compared with the current parameter condition. Achieve these reductions simultaneously is unattainable.

(3) To simultaneously achieve better results for all three objective functions, a balanced optimal point is obtained. By adjusting parameters such as decreasing the rear suspension initial gas pressure and damping valve orifice and slightly increasing the initial volume for both the front and rear suspension, which result in higher suspension stroke, the RMS values of cabin vertical acceleration, chassis roll angle, and chassis pitch angle can be reduced by 4%, 19%, and 29%, respectively. However, changes in the damping valve and maximum suspension stroke require design modifications and cannot be easily implemented in the current suspension.

(4) The 4% reduction in cabin vertical acceleration RMS (1.97 m/s² to 1.89 m/s²) is not significant, indicating that the current HPS parameters are already close to optimal for this objective function. Thus, whether through field adjustments or suspension design changes, a significant reduction in cabin acceleration to meet standard limits is not expected. Therefore, besides the HPS parameters study, it is necessary to study the road quality to evaluate its influence on cabin acceleration and determine the road class for which the standard limit can be achieved. The study and implementation of active HPS can also help to reduce vibration to levels within standards.

6. ACKNOWLEDGEMENTS

This work has been supported by a research project financed by Vale SA. The authors are also thankful to Eng. Maxuel Teixeira, from Sotreq, for his technical assistance during the development of this work. Finally, the financial support from CAPES is acknowledged.

7. REFERENCES

Ali, D., and Frimpong, S. (2018). Artificial intelligence models for predicting the performance of hydro-pneumatic suspension struts in large capacity dump trucks. *International Journal of Industrial Ergonomics.*

Baldi, M., and Meirelles, P. (2003). Analysis of Performance of a Hydropneumatic Suspension System. *COBEM 2003.*

Bauer, W. Hydropneumatic Suspension Systems. *Springer*. 2011.

Brasil, Ministério do Trabalho e Previdência, *Norma Regulamentadora No.9* – Avaliação e Controle das Exposições Ocupacionais a Agentes Físicos, Químicos e Biológicos, 2021.

Deb., K. (2011). Multi-Objective Optimization Using Evolutionary Algorithms: An Introduction. *KanGAL Report.*

Dindarloo, S. (2016). Dynamic impact of ageing dump truck suspension systems on whole-body vibrations in high-impact shovel loading operations.

Fossati, G., and Miguel, L. (2016). Multi-objective Optimization of a Vehicle's Dynamic Response to Excitations caused by a Road Profile through a Meta-Heuristic Algorithm. *CILAMCE 2016.*

ISO 2631-1, Mechanical vibration and shock - Evaluation of human exposure to whole-body vibration, Part I: General Requirements. *ISO (1997).*

ISO 8608, Mechanical vibration - Road surface profiles - Reporting of measured data. *ISO (2016).*

Kansake, B. (2019). Multi-body dynamic and finite element modeling of ultra-large dump truck-haul road interactions for machine health and haul road structural integrity.

Long, L. X., Ha, D. V., Quynh, L. V., Cuong, B. V., and Niem, V. T. (2021). Effect of operating conditions on a heavy truck ride comfort with hydro-pneumatic suspension system. *ICECAE 2021.*

Mitra, A., Desai, G., Patwardhan, S., Shirke, P., Kurne, W., and Banerjee, N. (2015). Optimization Of Passive Vehicle Suspension System By Genetic Algorithm. *Procedia Engineering.*

Oscarsson, M. (2015). A Hydropneumatic Suspension Parameter Study on Heavy Multi-Axle Vehicle Handling. *Royal Institute of Technology.*

Prem, H. (1998). Off-Highway Mine Haul Truck Dynamics Simulation. *SAE TECHNICAL PAPER SERIES.*

The Mathworks Inc. (2022). Optimization Toolbox version: 9.4 (R2022b), Natick, Massachusetts: *The MathWorks Inc.*

Thomann, J., and Eichfelder. G. (2019) Representation of the Pareto Front for heterogeneous multi-objective optimization. *J. Appl. Numer. Optim. 1.*

Westhuizen, S., and Els, P. (2015). Comparison of different gas models to calculate the spring force of a hydropneumatic suspension. *University of Pretoria.*

Wu, W., Tang, H., Zhang, S., Hu, L., and Zhang, F. (2020). High-Precision Dynamics Characteristic Modeling Method Research considering the Influence Factors of Hydropneumatic Suspension. *Hindawi, Shock and Vibration.*

Zhao, H., Wang, G., Lv, W., Cao, Y., and Li, X. (2018). Optimization of hydropneumatic suspension for articulated wheel loader based on kriging model and particle swarm algorithm. *Advances in Mechanical Engineering.*

8. RESPONSIBILITY NOTICE

The authors are the only responsible for the printed material included in this paper.